Factoring out non-decision time in choice RT data: supplemental information

Stijn Verdonck and Francis Tuerlinckx
Faculty of Psychology and Educational Sciences
KU Leuven, University of Leuven

Simulation study

For the details on the simulation study, we refer to the main text. In Figures 1,2,3 below we present the recovery results of all diffusion model parameters as listed in Table 1. In each figure we show the results for a single non-decision pdf scenario's, and three different sample sizes.

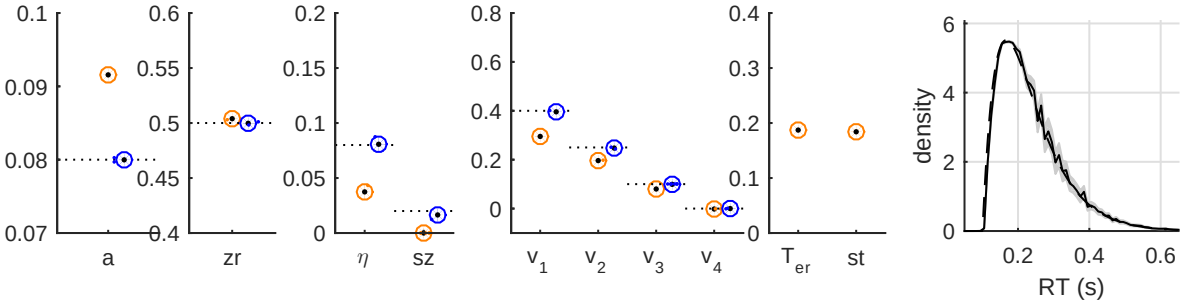

(a) recovery diffusion model parameters for 10^6 observations per condition

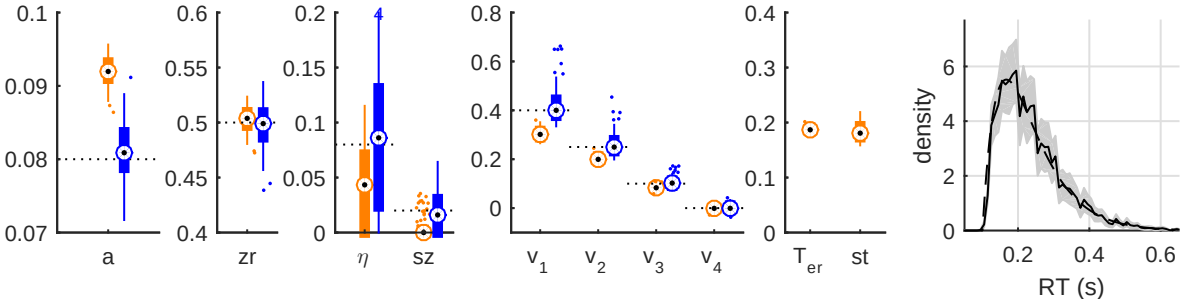

(b) recovery diffusion model parameters for 1000 observations per condition

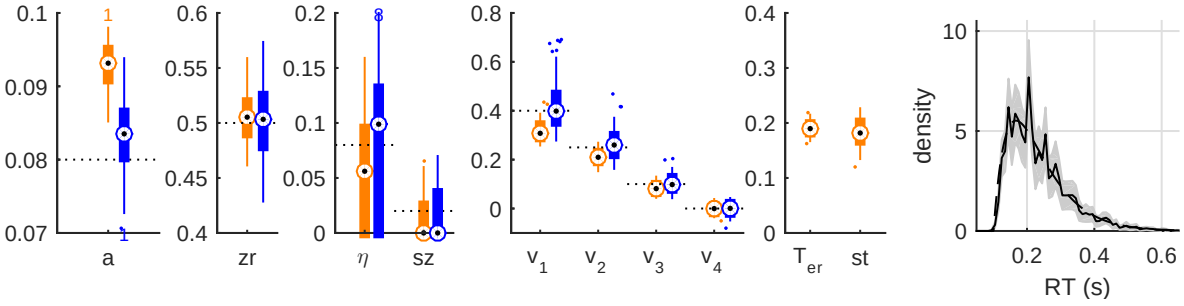

(c) recovery diffusion model parameters for 300 observations per condition

Figure 1. Recovery results for a right skewed non-decision pdf scenario. The three panels (a), (b), and (c) refer to three different sample sizes: 10^6, 1000 and 300 per condition. Each panel shows the estimates of the diffusion model parameters common to both the classical analysis (orange) and the D*M analysis (blue): boundary separation a, relative bias zr, drift rate variability η, starting point variability sz and the four drift rates v_1, v_2, v_3, v_4. In addition, the estimated T_{er} and st (mean and width of the uniform non-decision time distribution) for the classical analysis are shown. The rightmost figure contains the true (dashed line) and estimated (solid line) non-decision time pdf based on the D*M analysis.

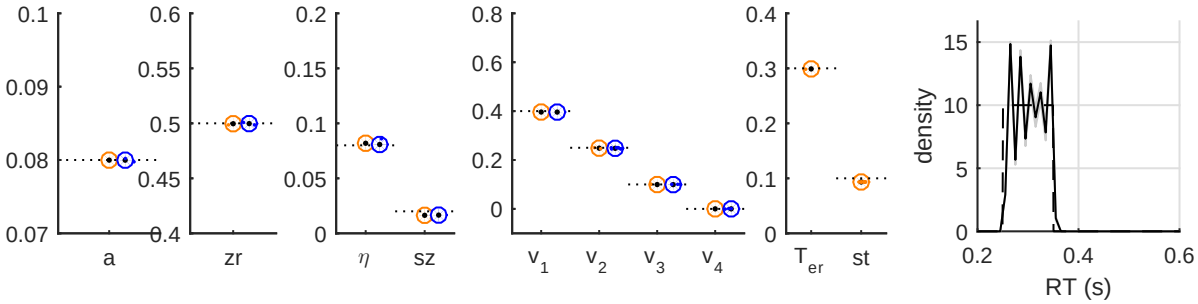

(a) recovery diffusion model parameters for 10^6 observations per condition

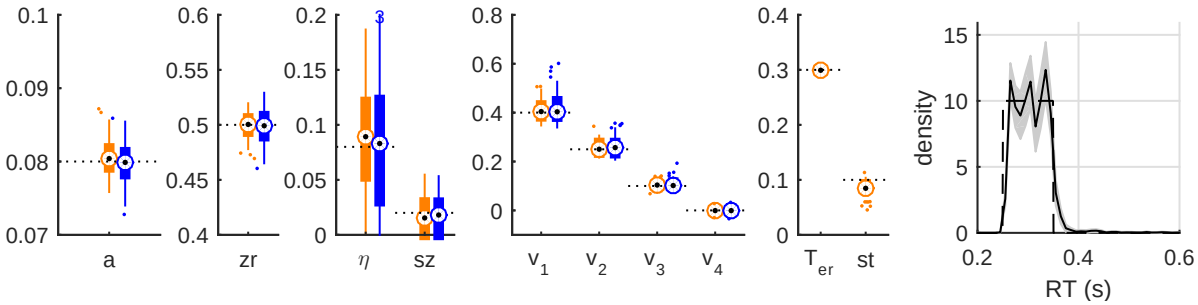

(b) recovery diffusion model parameters for 1000 observations per condition

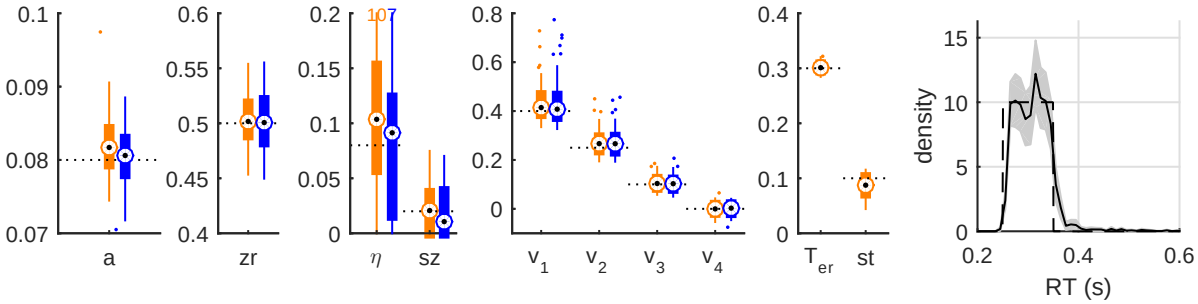

(c) recovery diffusion model parameters for 300 observations per condition

Figure 2. Recovery results for a uniform non-decision pdf scenario. The three panels (a), (b), and (c) refer to three different sample sizes: 10^6, 1000 and 300 per condition. Each panel shows the estimates of the diffusion model parameters common to both the classical analysis (orange) and the D*M analysis (blue): boundary separation a, relative bias zr, drift rate variability η, starting point variability sz and the four drift rates v_1, v_2, v_3, v_4. In addition, the estimated T_{er} and st (mean and width of the uniform non-decision time distribution) for the classical analysis are shown. The rightmost figure contains the true (dashed line) and estimated (solid line) non-decision time pdf based on the D*M analysis.

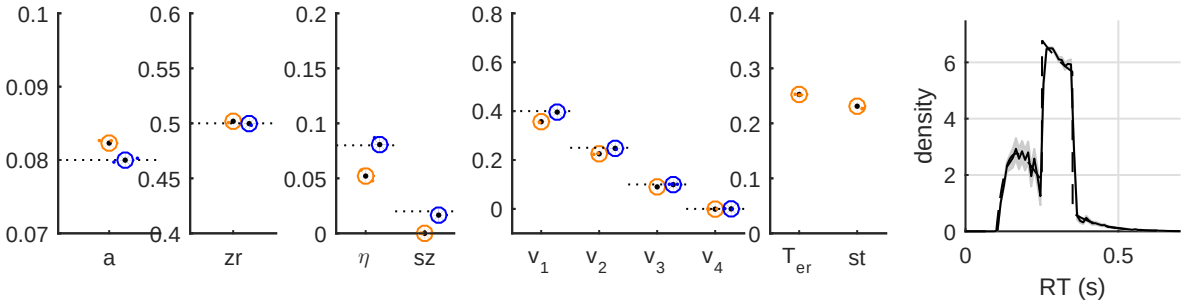

(a) recovery diffusion model parameters for 10^6 observations per condition

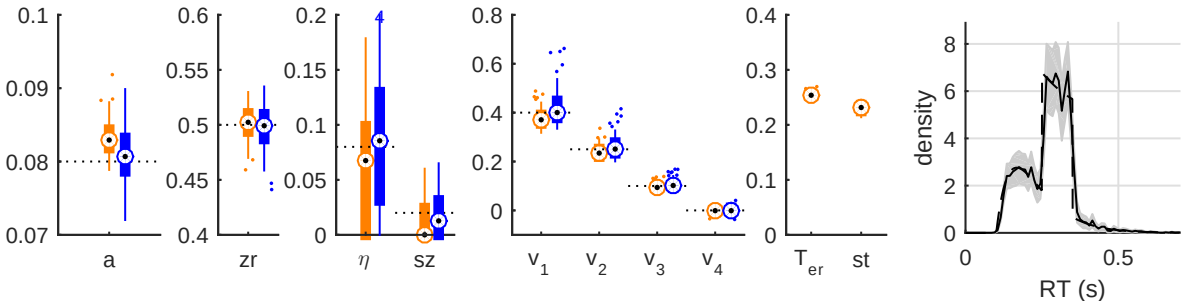

(b) recovery diffusion model parameters for 1000 observations per condition

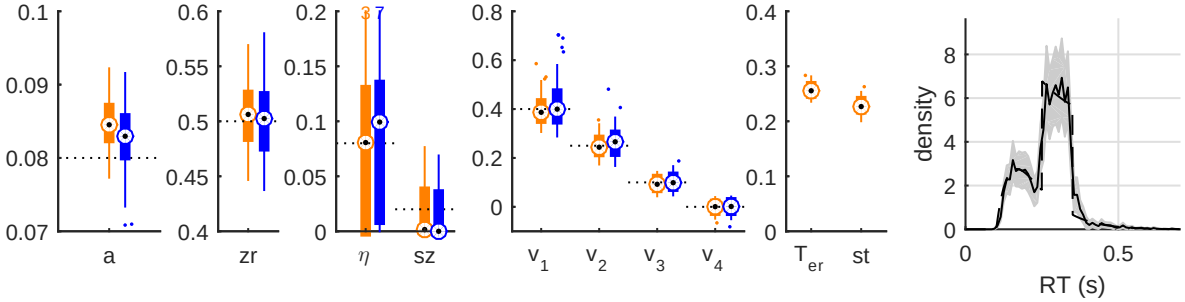

(c) recovery diffusion model parameters for 300 observations per condition

Figure 3. Recovery results for a bimodal non-decision pdf scenario. The three panels (a), (b), and (c) refer to three different sample sizes: 10^6, 1000 and 300 per condition. Each panel shows the estimates of the diffusion model parameters common to both the classical analysis (orange) and the D*M analysis (blue): boundary separation a, relative bias zr, drift rate variability η, starting point variability sz and the four drift rates v_1, v_2, v_3, v_4. In addition, the estimated T_{er} and st (mean and width of the uniform non-decision time distribution) for the classical analysis are shown. The rightmost figure contains the true (dashed line) and estimated (solid line) non-decision time pdf based on the D*M analysis.

Application 1: A diffusion application of choice bias

In Figure 4 we present the full set of results (for all parameters) of the traditional and D*M diffusion model fits to the data from Mulder, Wagenmakers, Ratcliff, Boekel, and Forstmann (2012).

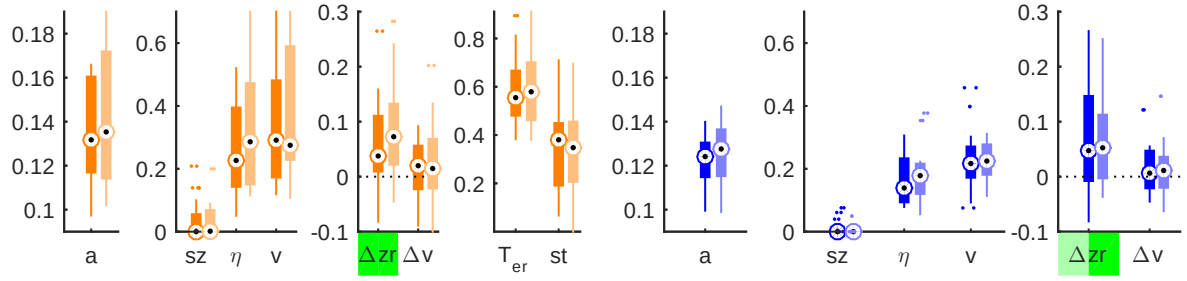

(a) traditional estimates

(b) D*M estimates

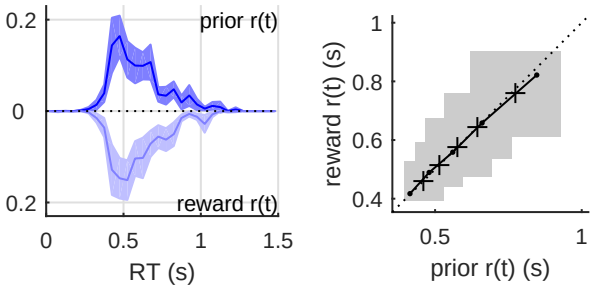

(c) non-decision pdfs

(d) Q-Q plot non-decision pdfs

Figure 4. Application 1: Parameter estimates of a diffusion model analysis of choice bias for 20 participants. The first two panels show the estimates of all decision model parameters (boundary separation a, inter-trial variability of bias sz, inter-trial variability of drift rate η and effects of bias on starting point Δzr and drift rate Δv), obtained with either the traditional (a, in orange, with the additional non-decision time parameters mean non-decision time T_{er} and inter-trial variability of non-decision time st) or D*M method (b, in blue). For each of the two panels, the darker box plots show the estimates for the elevated prior likelihood condition, the lighter plots for the larger potential pay-off condition. If for the group of participants Δzr or Δv is significantly different from 0 (two-sided sign test), this is indicated with a green ($p < 0.001$) or light green ($p < 0.01$) marking of the label. Panel (c) shows the non-decision time densities inferred from the D*M estimates in panel (b). The densities for the elevated likelihood condition are shown in the upper half of the plot and those for the larger potential pay-off condition are shown, mirrored, in the lower half. The solid lines show the mean non-decision pdfs across participants, the lighter areas display the double standard error interval. Panel (d) is a quantile-quantile plot of the data in panel (c), and is better suited to look at the differences between the non-decision pdfs from the two conditions. The grey area represents a 95% confidence interval of the mean quantile-quantile values (black crosses).

Application 2: A diffusion application of post-error slowing

In the figures below, we present the full set of results (for all parameters) of the traditional (Figures 5,7) and D*M (Figure 6) diffusion model fits to the data from Dutilh et al. (2011).

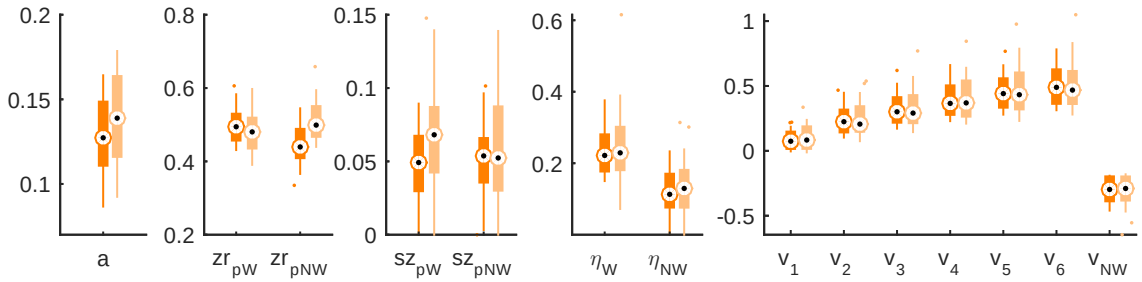

(a) decision model estimates

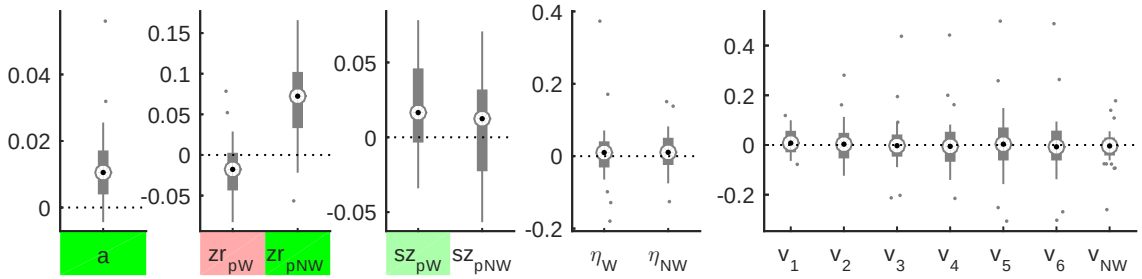

(b) decision model differences

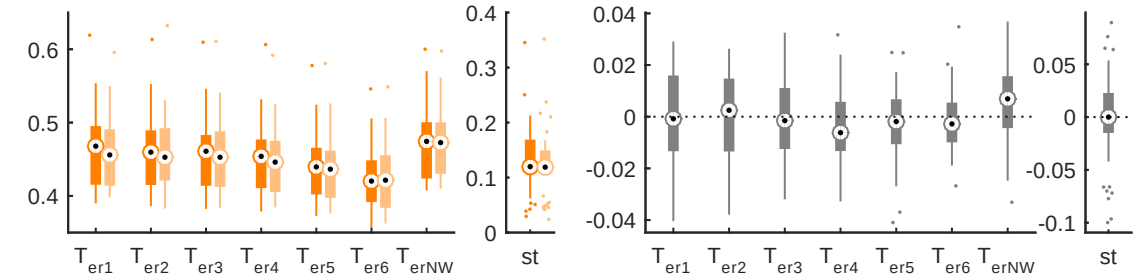

(c) non-decision estimates

(d) non-decision differences

Figure 5. Application 2: Estimation results of a traditional diffusion model analysis of post-error slowing for 39 participants. Panel (a) shows the traditional estimates for boundary separation a, relative bias after a word or non-word error trial (zr_{pW} and zr_{pNW}), inter-trial variability of bias after a word or non-word error trial (sz_{pW} and sz_{pNW}), inter-trial variability of drift rate for words and non-words (η_W and η_{NW}), and the drift rates for six different word types and non-words ($v_1, ..., v_6$ and v_{NW}), for both the post-correct condition (darker box plots) and the post-error condition (lighter box plots). Panel (b) shows the within-person differences between post-error and post-correct conditions of the parameters in panel (a). Statistically significant effects for the differences (two-sided sign test) are indicated with a green/red ($p < 0.001$) or light green/light red ($p < 0.01$) marking of the label (green means a positive effect or a larger value post-error compared to post-correct, red a negative effect or a smaller value post-error compared to post-correct). Panel (c) shows the estimates of the uniform non-decision time distributions: the mean per stimulus type ($T_{er1}, T_{er2}, T_{er3}, T_{er4}, T_{er5}, T_{er6}$ and T_{erNW}) and the common width st. Panel (d) shows the within-person differences between post-error and post-correct conditions of the parameters in panel (c).

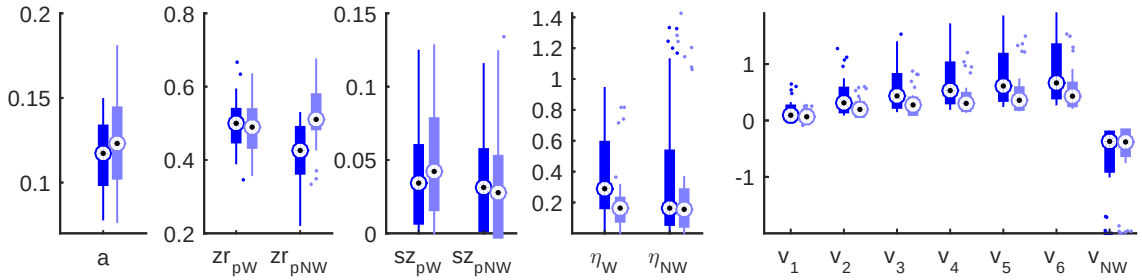

(a) decision model estimates

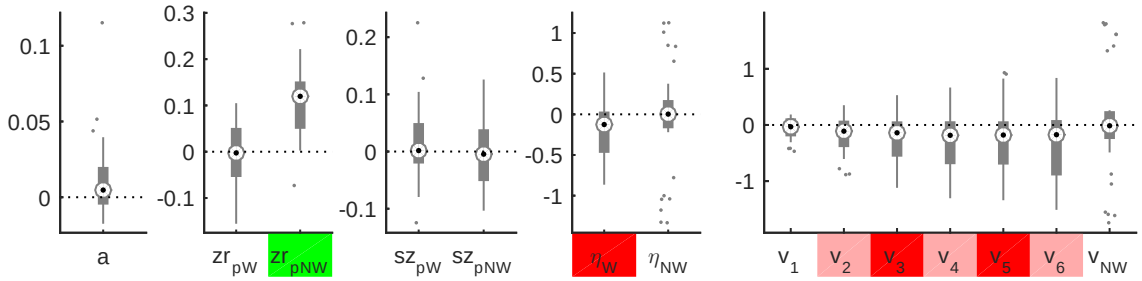

(b) decision model differences

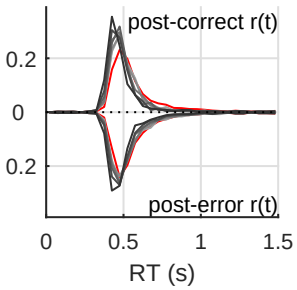

(c) non-decision pdfs

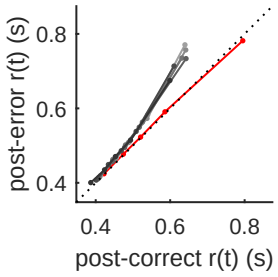

(d) Q-Q plot non-decision pdfs

Figure 6. Application 2: Estimation results of a D*M diffusion model analysis of post-error slowing for 39 participants. Panel (a) shows the D*M estimates for boundary separation a, relative bias after a word or non-word error trial (zr_{pW} and zr_{pNW}), inter-trial variability of bias after a word or non-word error trial (sz_{pW} and sz_{pNW}), inter-trial variability of drift rate for words and non-words (η_W and η_{NW}), and the drift rates for six different word types and non-words ($v_1, ..., v_6$ and v_{NW}), for both the post-correct condition (darker box plots) and the post-error condition (lighter box plots). Panel (b) shows the within-person differences between post-error and post-correct conditions of the parameters in panel (a). Statistically significant effects for the differences (two-sided sign test) are indicated with a green/red ($p < 0.001$) or light green/light red ($p < 0.01$) marking of the label (green means a positive effect or a larger value post-error compared to post-correct, red a negative effect or a smaller value post-error compared to post-correct). Panel (c) shows the participant averaged non-decision time densities inferred from the D*M estimates, separately for all six different word types (black) and non-words (red). The non-decision time densities of the post-correct condition are shown in the upper half, those of the post-error condition are shown, mirorred, in the lower half. Panel (d) is a quantile-quantile plot of the data in panel (c), and is better suited to look at the differences between the non-decision time densities from the two conditions. (Because of the many non-decision time pdfs, no confidence intervals are shown in panels (c) and (d).)

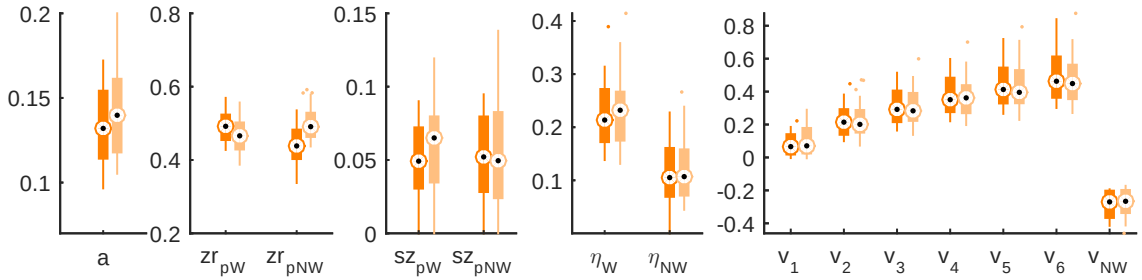

(a) decision model estimates

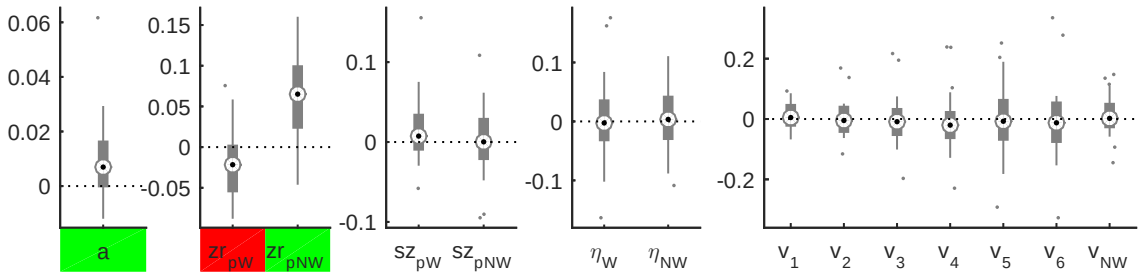

(b) decision model differences

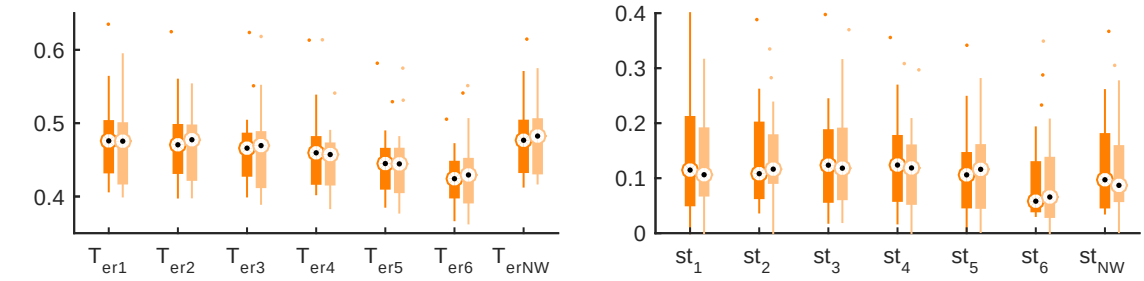

(c) non-decision model estimates

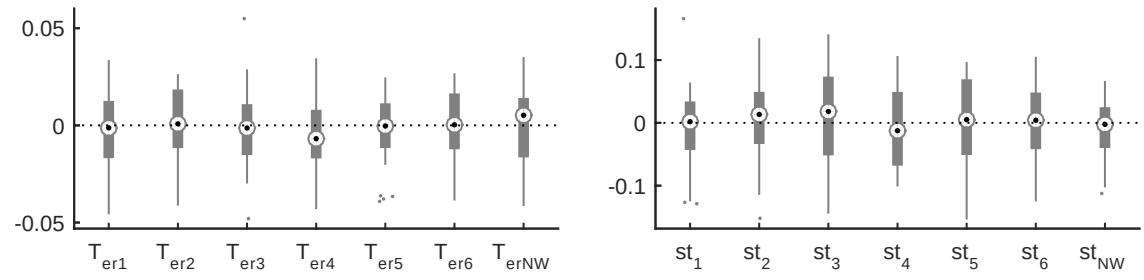

(d) non-decision model differences

Figure 7. Application 2: Estimation results of a traditional diffusion model analysis of post-error slowing for 39 participants, with separate inter-trial variabilities of non-decision time for different stimulus types. Panel (a) shows the traditional estimates for boundary separation a, relative bias after a word or non-word error trial (zr_{pW} and zr_{pNW}), inter-trial variability of bias after a word or non-word error trial (sz_{pW} and sz_{pNW}), inter-trial variability of drift rate for words and non-words (η_W and η_{NW}), and the drift rates for six different word types and non-words ($v_1, ..., v_6$ and v_{NW}), for both the post-correct condition (darker box plots) and the post-error condition (lighter box plots). Panel (b) shows the within-person differences between post-error and post-correct conditions of the parameters in panel (a). Statistically significant effects for the differences (two-sided signtest) are indicated with a green/red ($p < 0.001$) or light green/light red ($p < 0.01$) marking of the label (green means a positive effect or a larger value post-error compared to post-correct, red a negative effect or a smaller value post-error compared to post-correct). Panel (c) shows the estimates of the uniform non-decision time distributions: the mean per stimulus type ($T_{er1}, T_{er2}, T_{er3}, T_{er4}, T_{er5}, T_{er6}$ and T_{erNW}) and the width per stimulus type ($st_1, st_2, st_3, st_4, st_5, st_6$ and st_{NW}). Panel (d) shows the within-person differences between post-error and post-correct conditions of the parameters in panel (c).

Application 3: A diffusion application of task switching costs

In the figures below, we present the full set of results (for all parameters) of the traditional and D*M diffusion model fits to the data from Schmitz and Voss (2012). In Figure 8, task-switching trials are compared to pure task trials; in Figure 8, task-repeating trials are compared to pure task trials.

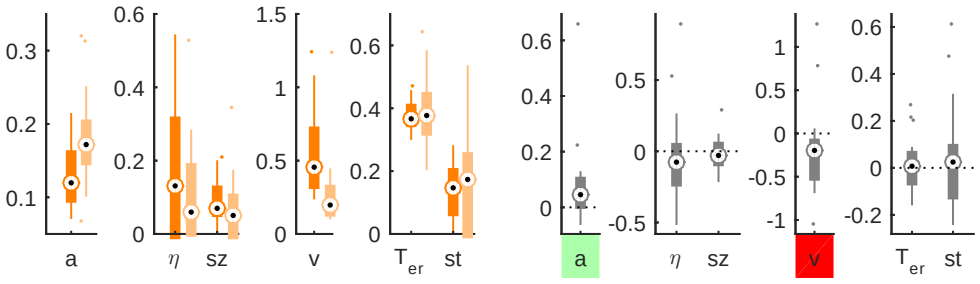

(a) traditional estimates (b) traditional differences

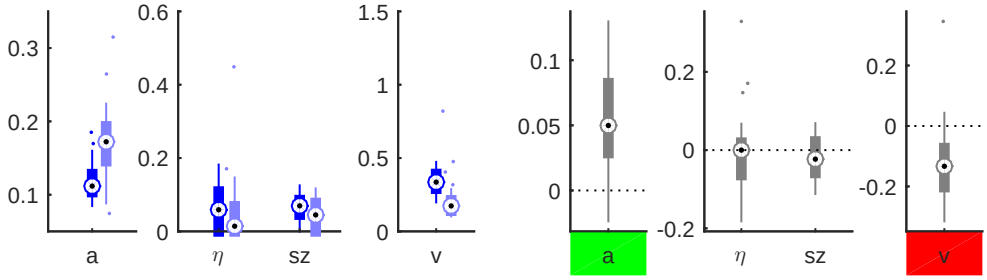

(c) D*M estimates (d) D*M differences

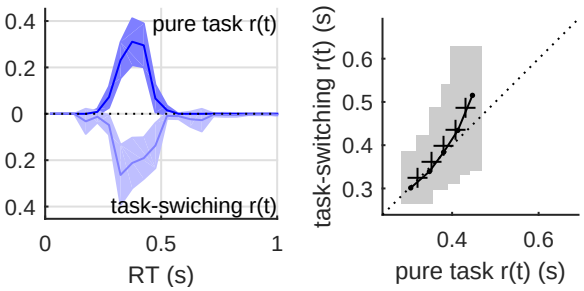

(e) non-decision pdfs (f) Q-Q plot non-decision pdfs

Figure 8. Application 3: Estimation results of a diffusion model analysis of task switching costs for 24 participants. Panel (a) shows the traditional estimates of all diffusion model parameters (boundary separation a, inter-trial variability of drift rate η, inter-trial variability of bias sz, drift rate v, uniform non-decision time distribution mean T_{er} and width st), for both the task-switching trials (lighter box plots) and the pure task trials (darker box plots). Panel (b) shows the within-person differences between task-switching and pure task conditions of the parameters in panel (a). Statistically significant effects for the differences (two-sided sign test) are indicated with a green/red ($p < 0.001$) or light green/ light red ($p < 0.01$) indicator (green means a larger parameter value in the task switch condition compared a pure task condition, red means smaller values). Panels (c) and (d) are the respective D*M versions of panels (a) and (b). Panel (e) shows the participant averaged non-decision time densities inferred from the D*M estimates. The non-decision time densities of the pure task condition are shown in the upper half of the plot, those of the task-switching trials are shown, mirrored, in the lower half. The solid lines show the mean non-decision pdfs across participants, the lighter areas display the double standard error interval. Panel (f) is a quantile-quantile plot of the data in panel (e), and is better suited to look at the differences between the non-decision pdfs from the two conditions. The grey area represents a 95% confidence interval of the mean quantile-quantile values (black crosses).

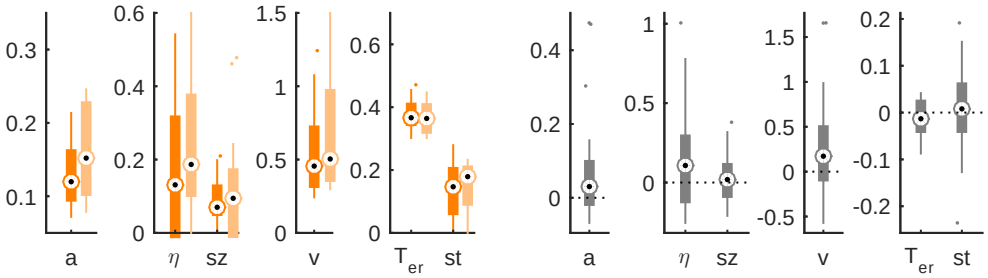

(a) traditional estimates

(b) traditional differences

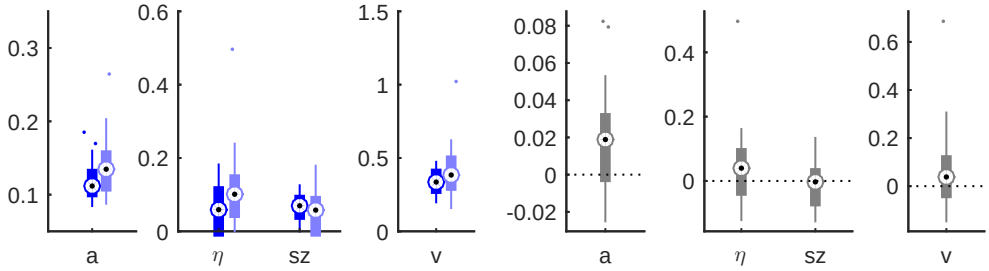

(c) D*M estimates

(d) D*M differences

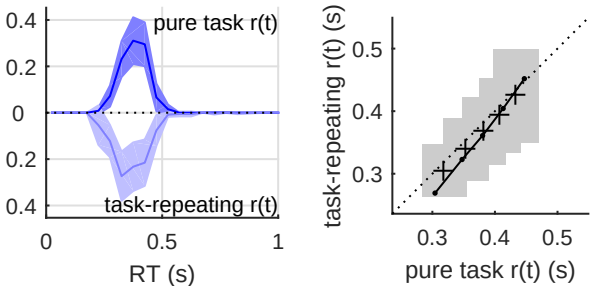

(e) non-decision pdfs

(f) Q-Q plot non-decision pdfs

Figure 9. Application 3: Estimation results of a diffusion model analysis of task switching costs for 24 participants. Panel (a) shows the traditional estimates of all diffusion model parameters (boundary separation a, inter-trial variability of drift rate η, inter-trial variability of bias sz, drift rate v, uniform non-decision time distribution mean T_{er} and width st), for both the task-repeating trials (lighter box plots) and the pure task trials (darker box plots). Panel (b) shows the within-person differences between task-switching and pure task conditions of the parameters in panel (a). Statistically significant effects for the differences (two-sided sign test) are indicated with a green/red ($p < 0.001$) or light green/ light red ($p < 0.01$) indicator (green means a larger parameter value in the task switch condition compared a pure task condition, red means smaller values). Panels (c) and (d) are the respective D*M versions of panels (a) and (b). Panel (e) shows the participant averaged non-decision time densities inferred from the D*M estimates. The non-decision time densities of the pure task condition are shown in the upper half of the plot, those of the task-switching trials are shown, mirrored, in the lower half. The solid lines show the mean non-decision pdfs across participants, the lighter areas display the double standard error interval. Panel (f) is a quantile-quantile plot of the data in panel (e), and is better suited to look at the differences between the non-decision pdfs from the two conditions. The grey area represents a 95% confidence interval of the mean quantile-quantile values (black crosses).

References

Dutilh, G., Vandekerckhove, J., Forstmann, B. U., Keuleers, E., Brysbaert, M., & Wagenmakers, E.-J. (2011, November). Testing theories of post-error slowing. *Attention, Perception, & Psychophysics*, *74*(2), 454–465. doi: 10.3758/s13414-011-0243-2

Mulder, M. J., Wagenmakers, E.-J., Ratcliff, R., Boekel, W., & Forstmann, B. U. (2012, February). Bias in the brain: A diffusion model analysis of prior probability and potential payoff. *The Journal of Neuroscience*, *32*(7), 2335–2343. doi: 10.1523/JNEUROSCI.4156-11.2012

Schmitz, F., & Voss, A. (2012). Decomposing task-switching costs with the diffusion model. *Journal of Experimental Psychology: Human Perception and Performance*, *38*(1), 222–250. doi: 10.1037/a0026003